Experimental and Numerical Investigation of the Axial Behavior of Connection in CFST Diagrid Structures[*]

HAN Xiaolei (韩小雷), HUANG Chao (黄 超)[**], JI Jing (季 静), WU Jianying (吴建营)

State Key Laboratory of Subtropical Architecture Science, School of Civil and Transportation Engineering, South China University of Technology, Guangzhou 510640, China

Abstract: Concrete filled steel tubular (CFST) diagrid structures usually have connections intersected by four oblique CFST columns. In order to investigate the performance, capacity and failure mechanism of the connections, two 1/5.5-scale specimens were tested under monotonic axial loading. The parameters in the study were the separation angle between columns. While the test was being conducted, the deflection, stress, failure pattern and capacity of the specimens were obtained and analyzed. In addition, the connection was analyzed using the general finite element analysis (FEA) software ABAQUS, with the purpose of investigating the mechanism, the weakness, the distribution of stress, and the bearing capacity of the connections. Experimental and numerical results indicate that the connecting separation angles resulted in the difference of failure modes and the mechanical behavior of the connections was similar to the behavior of CFST short columns.

Key words: diagrid structure; connection; concrete filled steel tubular (CFST); nonlinear analysis; finite element analysis (FEA)

Introduction

Recently, diagrid structures have emerged as both structurally efficient and architecturally significant in tall buildings, especially super high-rise buildings with height above 150 m, such as the Swiss Re Building in London, the Hearst Headquarters in New York, the Ministry of Foreign Affairs Building in Qatar, Guangzhou West Tower (432 m), etc. The use of diagrid structures for effective lateral and torsional stiffness has generated interest from structural scholars and designers of tall buildings[1-2].

According to Kyoung-sun Moon et al[1], the geometry

of a diagrid structure acquires structural members minimized in practical use[1]. Therefore, as a composite structure that takes advantage of both concrete and steel, concrete filled steel tubular (CFST) components are suitable for diagrid structural members. CFST structures are used in many applications and have become more widespread in recent decades. Research on CFST structures has been conducted in China, Japan, the United States and other countries[3-9].

CFST diagrid structures usually have connections comprised of four obliquely intersecting CFST columns. As the cross-sectional area at the connection is reduced to that of each CFST column, the connection details become the key link in the structural design. There appears to have been no systematic investigation of these details. This paper proposes a new connection and two 1/5.5-scale specimens were tested under monotonic axial loading. The deflection, stress, failure modes and capacity of the specimens are experimentally

obtained and analyzed. In addition, it analyzed the connection using the general finite element analysis software ABAQUS, with the purpose of investigating the mechanism, the weakness, the distribution of stress, the bearing capacity and the ductility performance of the connections. As a result, some design recommendations of the connections are proposed based on the previous analysis.

1　Experiment Investigation

Two 1/5.5-scale specimens of a CFST connection in a diagrid structure were tested under monotonic axial loading. The purpose of the study was (1) to investigate the failure modes of the connections, (2) to verify the ultimate capacity of the connection under axial loading, (3) to measure the steel tube's strain distribution, the axial deformation and the lateral deflection of the specimens through the entire test procedure, and (4) to assess the effectiveness of the connection in practical use.

1.1　Test Specimens and parameters

The test parameters were the separation angle between columns: 20° and 35°. The details of each specimen are shown in Fig. 1.

Each connection consists of 4 intersecting CFST columns which were welded fully to an elliptical plate. In addition, two steel sleeve barrels with 10 mm wall thickness were welded on the loading end while a 20 mm plate was welded on the fixed end.
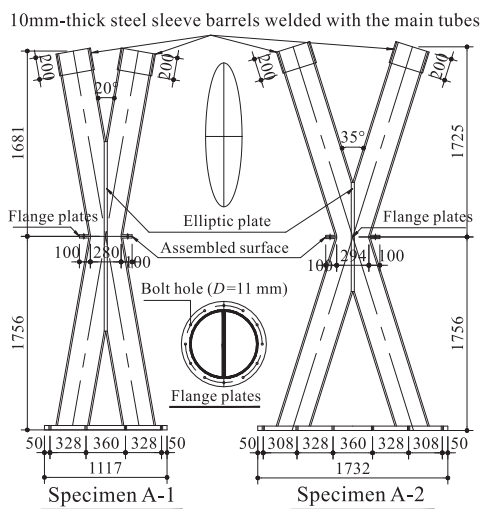

Fig. 1　Specimen details (unit: mm)

Steel tubes and plates were manufactured using mild structural steel with a nominal yield stress of 275 MPa. The material properties of the steel tubes and plates were obtained from tensile tests of coupons taken from each steel plate before manufacturing. The concrete grade of all specimens was C60. Compression tests were carried out on three cube specimens (150 mm in lengths) to determine the compressive strength of the concrete.

1.2　Test procedure

Two sets of loading systems including a 10 000 kN hydraulic jack and a related sensing unit were used to apply the axial load on each column in turn. Since the columns intersected obliquely, each of the systems had a support comprised of 2 steel plates welded on 4 rib stiffeners so that the hydraulic jacks could apply axial loads on the specimens. In addition, a self-equilibrating steel loading device with a capacity of 20 000 kN was designed to bear the counterforce generated by the jacks (Fig. 2).

Fig. 2　Test setup

A detailed instrumentation procedure was used to measure the strains and deformations. The steel tubes in the connections and the columns were instrumented with 84 strain gauges and 20 dial gauges connected to a computer data acquisition system to record their values. Any one of three conditions concluded the test: (1) the ultimate capacity decreased to 85% of the maximum, (2) the maximum deformation reached 90mm, or (3) obvious features of failure occurred in the specimens.

2　Experimental Results

2.1　Failure modes

The pertinent measurements and observations extracted from the experiment included failure modes,

load-steel tube strain and load-deflection results.

It was observed that the failure modes could be divided into two types. For the specimens with a separation angle equal to 20°, the failure was due to the tube bulging within the connection zone (Fig. 3a). It produced some Lüders slip lines (Fig. 3b) along the surface of the tubes. In addition, bending in-plane occurred in some part of the specimens. Whereas for the specimens with a separation angle equal to 35°, the failure was due to the tube bulging outside the connection zone. It also produced some Lüders slip lines along the surface of tube near both the support ends and loading ends (Fig. 3c). Bending in plane occurred near the support ends.

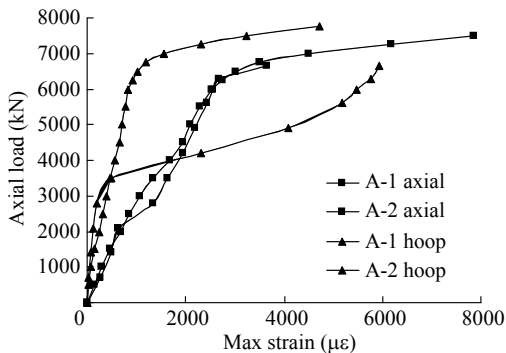(a) Bulging at the center of the connection   (b) Lüders slip lines in part of tube   (c) Bulging at the support end
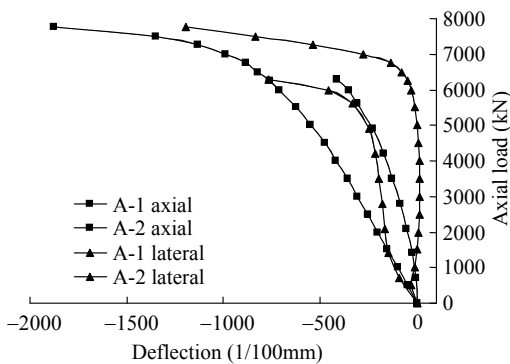
Fig. 3   Failure modes

2.2   Load-steel strain and load-deflection

The axial load-strain curves of specimen A-1 and A-2 are illustrated in Fig. 4a and their load-deflection responses are illustrated in Fig. 4b.

(a) Axial load-maximum strain

(b) Axial load-deflection

Fig. 4   Load-steel strain and load-deflection curves

The curves of Figs 4a illustrate the point of steel yielding, the maximum load and the ductility of the element. It can be seen that the trend of the curves are corresponds well with those of short CFST columns in some previous research[3-5]. The five significant events for each specimen during testing are as follows: (1) the steel tube was compressed in the axial direction while tensioned in the circular direction, and the axial strains increased faster than the hoop strains, (2) the axial and hoop strains continued increasing linearly until the axial strains reached 1600με, or the axial loads were below 3000kN-5000kN, (3) subsequently, the strains increased abruptly with a non-linear trend, which indicates that the steel tubes yield under a axial compression and a hoop tension stress, (4) although the tubes were in yield phase, the load could be increased until it reached 7250kN-7500kN due to the stress redistribution which occurred between the concrete and tubes, (5) when the load reached maximum load, steel bulging occurred in the central zone or the fixed end as described in section 2.1. Some Lüders slide lines also occurred along the surface of the tubes.

The curves of Fig. 4b illustrate that the axial deformation increased linearly until the load reached 6000kN, so that the axial stiffness of the connections is applicable to tall buildings. In addition, it can be seen that the deflection increased extremely fast after the tube stress achieves yield stress, which shows that the out-plane lateral stiffness of the connections is not as

good as the axial stiffness and lateral braces are necessary when applied to the high-rise structures.

2.3 Comparison and analysis of the ultimate axial loads

Referring to the specification for design of CFST structures (CECS 28:90)[10], assuming that the most disadvantageous cross section is the center section of the connection, the design value F can be calculated as follows:

$$F = A_c f_c \left(1 + \sqrt{\frac{f_s A_s}{f_c A_c}} + \frac{f_s A_s}{f_c A_c} \right) \tag{1}$$

where f_s, f_c stands for the design strength of steel and concrete, while A_s, A_c stands for the area of steel and concrete respectively. It is noteworthy that A_s is summed by the cross section area of the steel tubes and the elliptic plate.

Table 1 compares the design values and test results of the ultimate axial load at each single column of the connections. The actual axial capacities of the specimen A-1 and A-2 were 1.56 and 1.61 times the design values, thus the design strengths of the connections were reliable.

Table 1 Experimental results and design value of the connections

Speci-mens	Yield load (kN)	Elastic load (kN)	Ultimate load P (kN)	Design values F (kN)	Ratio of P/F
A-1	3500	4200	7250	4650	1.56
A-2	3500	4500	7500		1.61

3 Analytical Modeling

3.1 Constitutive modeling of materials

As the concrete failure was controlled by compressive stress, a microplane model M4 developed by professor Bažant were used as constitutive modeling of concrete[11-13]. M4 model could simulate the nonlinear axial, bending and shear behavior under different stress condition. The parameters for M4 in this paper were: E^0=35.0 GPa, v^0=0.18, k_1=2.2×10^{-4}, k_2=500.0, k_3=15.0, and k_4 = 150.0. Corresponding symbols were explained[12,13]. The constitutive relations of steel were described by bilinear stress-strain curves, with the tangent modulus of 206 GPa, the hardening modulus of 20.6 GPa, the yield stress of 275 MPa, and the ultimate stress of 490 MPa.

3.2 Connection models

Two solid FEA models were created to represent the connections. In recent years, advancements in FEA formulation have produced robust algorithms to deal with complex geometry, large deformation, plasticity, and contact interactions. The general-purpose FEA software ABAQUS was selected for this simulation. Due to symmetry, only a quarter of each specimen was analyzed. Symmetric boundary conditions were imposed on the two planes of symmetry, one longitudinal plane along the centerline of the elliptic plate and another one at the midheight of the tube and perpendicular to the elliptic plate. The FEA models of the two connections are shown in Fig. 5.
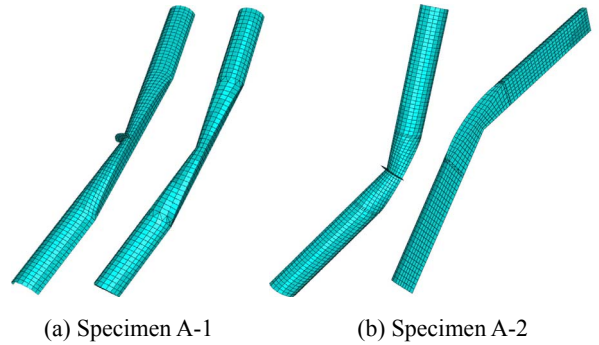

(a) Specimen A-1   (b) Specimen A-2

Fig. 5 Quarter models of steel tubes and core concrete

In the 3D models, eight-node isoparametric solid elements with reduced integration C3D8R were employed to model the core concrete, while four-node shell elements S4R were employed to model the steel tubes. The interaction between the core concrete and the steel tubes were simulated by a contact element with different normal and tangential behavior. This contact element defines the hard contact which prohibits element penetrate each other in the normal direction, and frictionate each other with friction coefficient μ = 0.30 in the tangential direction. The behavior of this contact element considered confined forces on the core concrete provided by tubes and axial friction between the two materials, was validated by plenty of test data.

3.3 Analytical result of the connections

As observed in the experimental work, the FEA model clearly demonstrates the axial behavior of the connections. Furthermore, because of the load sharing between

the core concrete and tube wall, the connection achieves a high load capacity. The comparison between the experimental results and FEA modeling results for the load-strain relationship is shown in Fig. 6.
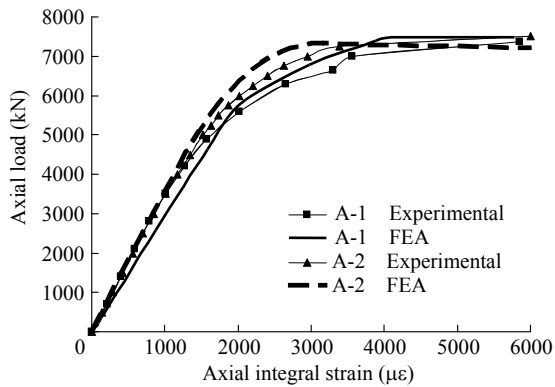

Fig. 6   Comparison on axial load-axial integral strain

The FEA models were slightly stiffer compared to the test results. In addition, the ultimate bearing capacity was slightly higher than experimental results. Figures 7 shows the Von Mises stress contours of different parts of the specimen A-1 and A-2 including the flange plates, the elliptic plate, the steel tubes and the core concrete. As the largest stress of A-1 appears at the center zone of the specimen, the weakness of smaller angled specimen is the connection zone. On the other hand, comparing Fig. 7g and Fig. 7h, it can be seen that the weakness of larger angled specimen is the zone outside center. In general, the FEA simulation is in good agreement with the experimental result. Further improvements to the FEA results could be achieved by introducing further refinements to the contact element properties, plasticity model, and geometric simplifications. This can be done by taking these factors into account: (1) better representation of stress-strain behavior for materials in the FEA model; (2) the effects of residual stress; and (3) imperfections originating from assembly of the tested specimens.

4   Discussion on the Mechanism of the Connections

According to previous research on CFST short columns, in the initial stages of loading of circular CFST columns subjected to axial load, Poisson's ratio for the concrete is lower than that for steel. Therefore a separation between the steel tube wall and the concrete core takes place. As the load increases, the longitudinal
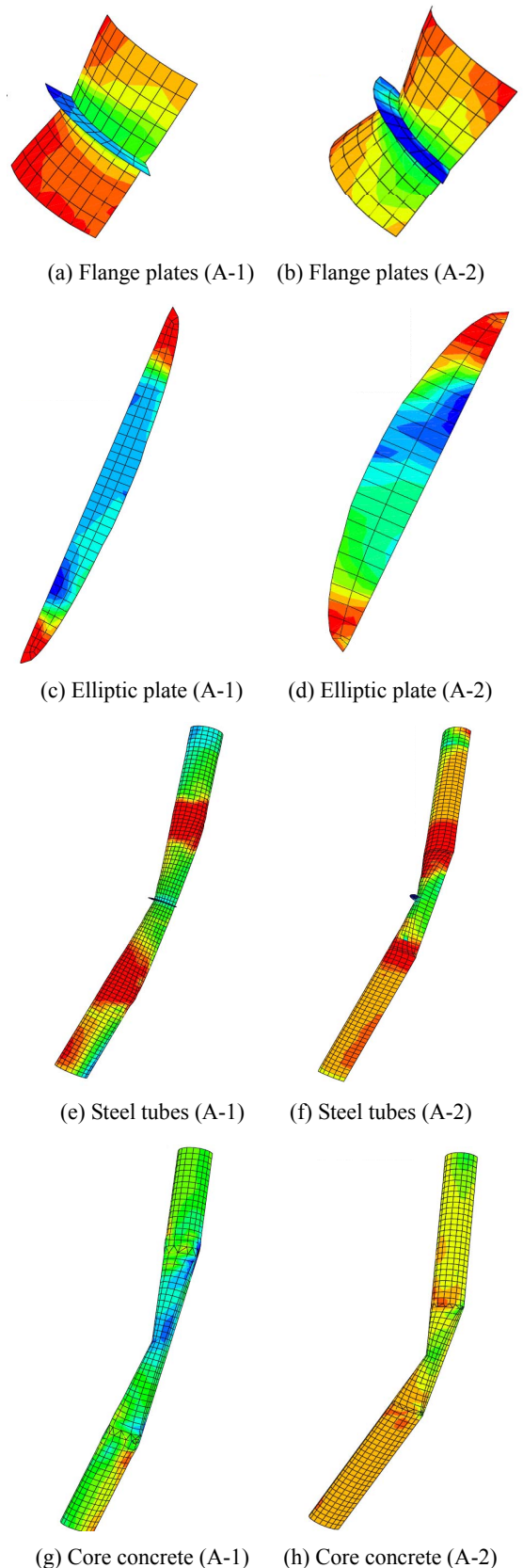

(a) Flange plates (A-1)   (b) Flange plates (A-2)

(c) Elliptic plate (A-1)   (d) Elliptic plate (A-2)

(e) Steel tubes (A-1)   (f) Steel tubes (A-2)

(g) Core concrete (A-1)   (h) Core concrete (A-2)

Fig. 7   Von Mises stress contours of the specimens (unit: MPa)

strain reaches a certain critical strain, and the lateral deformation of the concrete catches up with that of the steel tube. When the load increases further, a tensile hoop stress is developed in the steel tube, and the concrete core is subjected to triaxial compression. This phenomenon results in an increase of axial compressive load capacity. In this test, it was validated that the mechanical behavior of the connections was similar to the behavior of CFST columns.

5 Conclusions and Recommendations

The failure modes and bearing capacity of two connections were obtained from experimental and analytic results, which offers the basis of the structural design. The bearing capacity of both connection details can meet the values required by structural design. In fact, the ratios of the actual axial capacities to the design values of the connections were 1.56 and 1.61. The separation angle of the connections will result in failure modes. Smaller angled separation connection needs to be reinforced appropriately to adhere to the seismic design principle "stronger connection, weaker components" which was defined by current codes. In general, the FEA simulations are in good agreement with the experimental results. Therefore, both results can be substantiated to be correct and usable. Finally, the mechanical behavior of the connections was verified to be similar to the behavior of CFST short columns.

The behavior of the connections in CFST diagrid structures was studied under axial monotonic compression loads. The experimental program and numerical analysis were conducted on connections with a specific detail and two specific separation angles. Therefore, the conclusions may or may not be valid for other connections. Further research is also still needed on CFST oblique crossing connections with different details used in the field.

Acknowledgements

References

[1] Moon K S, Connor J J, Fernandez J E. Diagrid structural systems for tall buildings: Characteristics and methodology for preliminary design. *The Structural Design of Tall and Special Buildings*, 2007, **16**: 205-230.

[2] Zhou Jian, Wang Dasui. Performance research on high-rise diagonal frame structures. *Building Structure*, 2007, **37**(5): 87-91. (in Chinese)

[3] Hu H T, Huang C S, Wu M H, et al. Nonlinear analysis of axially loaded concrete-filled tube columns with confinement effect. *Journal of Structural Engineering*, 2003, **129**(10): 1322-1329.

[4] Roeder C W, Cameron B, Brown C B. Composite action in concrete filled tubes. *Journal of Structural Engineering*, 1999, **125**(5): 477-484.

[5] Xiao Y, He W, and Choi K K. Confined concrete-filled tubular columns. *Journal of Structural Engineering*, 2005 **131**(3): 488-497.

[6] Jarquio R V. Analytical method of predicting the ultimate strength of CFT columns. In: Proceedings of Structures Congress, ASCE. Nashville, Tennessee, USA, 2004: 1-10.

[7] Mohammad S. Non-linear evaluation of concrete filled tubular columns [Dissertation]. New Jersey Institute of Technology at Newark, NJ, 1997.

[8] Sakino K, Nakahara H, Morino S, et al. Behavior of centrally loaded concrete-filled steel-tube short columns. *Journal of Structural Engineering*, 2004, **130**(2): 180-188.

[9] Cai Shaohuai. Modern Steel Tube Confined Concrete Structures. 2nd Ed. Beijing: China Communications Press, 2007. (in Chinese)

[10] CECS 28:90, Specification for Design and Construction of Concrete-filled Steel Tubular Structures. Beijing, China, 1990. (in Chinese)

[11] Bažant Z P, Oh B H. Microplane model for progressive fracture of concrete and rock. *Journal of Engineering Mechanics*, 1985, **111**(4): 559-582.

[12] Bažant Z P, Caner F C, Carol I, et al. Microplane model M4 for concrete. I: Formulation with work-conjugate deviatoric stress. *Journal of Engineering Mechanics*, 2000, **126**(9): 944-953.

[13] Caner F C, Bažant Z P. Microplane model M4 for concrete. II: Algorithm and calibration. *Journal of Engineering Mechanics*, 2000, **126**(9): 954-961.